LA-UR -85-3447

Los Alamos National Laboratory is operated by the University of California for the United States Department of Energy under contract W-7405-ENG-36

LA-UR--85-3447

DE86 000800

TITLE: Applications of Carbon-13 and Sodium-23 NMR in the Study of Plants, Animal, and Human Cells

AUTHOR(S): L. O. Sillerud, J. W. Heyser, C. H. Han, M. W. Bitensky

SUBMITTED TO: Proceedings of the NATO Advanced Study Institute
Palermo, Sicily, August 1984, Publisher: D. Reidel, Boston

DISCLAIMER

Los Alamos National Laboratory
Los Alamos, New Mexico 87545

FORM NO 836 R4
ST NO 2629 5/81

APPLICATIONS OF CARBON-13 AND SODIUM-23 NMR IN THE STUDY OF PLANTS, ANIMAL, AND HUMAN CELLS

Laurel O. Sillerud, James W. Heyser Chung H. Han, and Mark W. Bitensky
Division, of Life Sciences, Los Alamos National Laboratory, University of California, Los Alamos, New Mexico 87545

0.0 ABSTRACT

Carbon-13 and sodium-23 NMR have been applied to the study of a variety of plant, animal and human cell types. Sodium NMR, in combination with dysprosium shift reagents, has been used to monitor sodium transport kinetics in salt-adapted, and non-adapted cells of P. milliaceum and whole D. spicata plants. The sodium content of human erythrocytes and leukemic macrophages was measured. Carbon-13 NMR was used to determine the structure and metabolism of rat epididymal fat pad adipocytes in real time. Insulin and isoproterenol-stimulated triacylglycerol turnover could be monitored in fat cell suspensions. [1-^{13}C] glucose was used as a substrate to demonstrate futile metabolic cycling from glucose to glycerol during lypolysis. Cell wall polysaccharide synthesis was followed in suspensions of P. milliaceum cells using [1-^{13}C] glucose as a precursor. These results illustrate the wide range of living systems which are amenable to study with NMR.

1.0 INTRODUCTION

In light of the relatively large cost of modern high-field NMR systems, especially those suitable for use on human patients, it is important to understand the reasons why the utility of NMR justifies its expense in applications to living systems. An examination of the available methods for the investigation of the interior of the body reveals that only a handful can give structural information in a non-invasive manner: these include NMR, x-ray, computed tomography, ultrasound, and neutron scattering. Other spectroscopic methods use probes of high energy or short wavelength which cause physical or chemical changes in cells. NMR is one of the only technologies that can provide functional information without the need for radiation, cell or tissue disruption, or damage to the system. In addition, it is selective for various nuclei in different chemical or biochemical environments and gives data in real time with respect to the integrity of chemical bonds.

A complete picture of the applicability of NMR to living systems must also include an exposition of limitations of the technology. While all of the major bionuclei have isotopes that have non-zero spin, and hence, give rise to NMR signals, these nuclei differ greatly in terms of their sensitivity, natural abundance, and biochemical concentrations in tissues of interest. Some, such as hydrogen, and phosphorus-31 have narrow signals due to the fact that they posess a nuclear spin of 1/2, while others such as sodium-23 and oxygen-17 are quadrupolar nuclei with much broader lines. Carbon-13 is present in nature at an abundance of 1.1% of all of the carbon so that signals from this nuclide will be difficult to obtain without the use of enrichment or large samples. This general lack of sensitivity limits NMR to the detection of only the most abundant chemical species. Furthermore, the width of a nuclear magnetic resonance signal increases as the correlation time of the nucleus decreases; this leads to the conclusion that NMR observes high-resolution signals from only the most mobile components of cells and tissues. In general these components are the small molecules such as glucose, metabolic precursors or products, free ions or mobile side chains on proteins or lipids. All modern NMR studies of living systems are done with the aid of signal averaging and Fourier transformation with finite pulse repetition rates. Consequently, the nuclear magnetization virtually never returns to equilibrium after the last pulse before the next is applied, and one must know the rate of spin relaxation in order to correct the observed signal intensities to obtain accurate measurements of the tissue concentrations of metabolites. Once these factors are taken into account in the design, execution, and analysis of an NMR experiment, the full substantial potential of NMR examination of living systems can be realized.

Our investigations to date have been directed at applications of NMR to living systems that have not been examined previously. There are active plant biotechnology and diabetes groups working at Los Alamos National Laboratory so that studies in these fields were chosen as initial demonstrations of the uses of NMR in new directions. Sodium toxicity is an important issue confronting all agricultural endeavors which utilize irrigation. We applied sodium-23 NMR at natural abundance to the study of the sodium content and tissue transport of salt tolerant monocotyledonous grasses of agricultural and economic importance in the American West and Southwest. We also used sodium-23 NMR, in combination with dysprosium-based anionic shift reagents, to measure the sodium content of normal human erythrocytes and human leukemic macrophages.

Carbon-13 NMR was chosen as the method by which the metabolism of adipose tissue could be monitored in order to assess the defects responsible for, and contributing to, diabetes. In this area Los Alamos National Laboratory is in the unique position of a lead laboratory with respect to the large-scale production of carbon-13. We have been producing carbon-13 at an isotopic enrichment of greater than 99% for the last 15 years for both internal and external use. At the same time, our National Stable Isotopes Resource has promoted the incorporation of this stable, spin 1/2, magnetic isotope into

biomolecules of interest to the NMR community. We have sought to use this C-13 in the study of the metabolic regulation of adipose tissue. We also have examined the biosynthesis of cellular polysaccharides in millet (Panicum miliaceum) cell suspensions using [1-^{13}C]-D-glucose as a metabolic precursor. Natural-abundance carbon-13 NMR is an alternative to the somewhat expensive enrichment that is done for metabolic studies. We illustrate an application of natural-abundance C-13 NMR to the study of hormone-stimulated lipolysis in adipocytes.

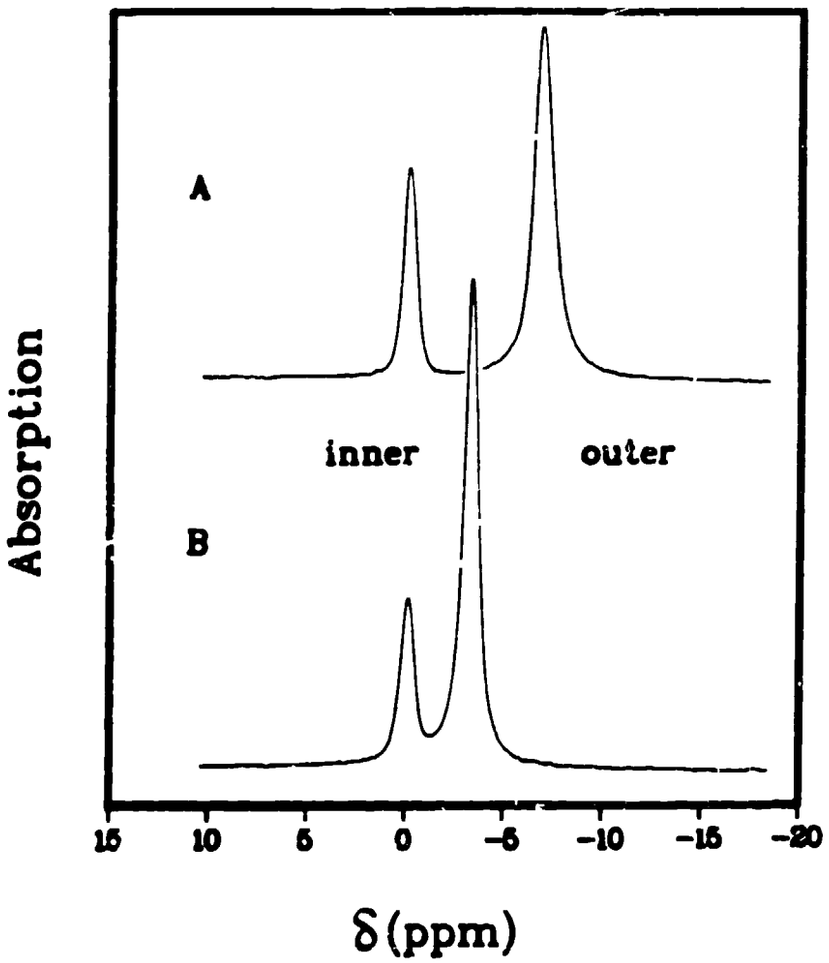

Fig. 1. Natural abundance sodium-23 NMR spectra of a suspension of millet cells, grown on 130 mM NaCl, in the presence of 5 mM DyTP at a temperature of 292K. (A) Cell spectrum taken for 3 min prior to the initiation of efflux. (B) Cell spectrum taken for 3 min commencing 90 min after the initiation of sodium efflux by means of a two-fold dilution of the exterior medium with sodium-free medium. Inner and outer here refer to the intracellular and extracellular sodium compartments, respectively.

2.0 SODIUM-23 NMR OF PLANT AND HUMAN CELLS AND WHOLE PLANTS

The cytosolic enzymes of many plant cells are inhibited by high intracellular concentrations of sodium. How certain plants deal with this sodium represents a key feature in their relative ability to grow in saline environments such as occur during the salinity increase accompanying prolonged irrigation of the soil with water which contains some dissolved salts. Sodium-23 NMR provides a rapid, non-invasive method for the determination of the amount, and distribution, of sodium ions in cells: data can be obtained with a time resolution of seconds, in real-time, without the need for extraction or disruption of the plant cells. Furthermore, efflux or influx time courses can be obtained in vivo from single samples of cells. The minimum concentration that can be measured is about 1 mM with a signal to noise ratio of about 10:1 in 1-2 min. The interior and exterior sodium signals from millet cells were separated with the aid of dysprosium (III) triphosphate (DyTP) (1,2) so that the sodium concentration in each compartment could be determined simultaneously. The DyTP was not taken up by the cells.

In order to follow changes in the amounts of sodium in the millet cells, we added 5 mM DyTP to the suspension and observed the intracellular and extracellular sodium-23 signals as a function of time. This amount of the shift reagent split the sodium resonance into two signals separated by about 7 ppm (Fig. 1) and about 1 ppm in width. The alterations in the sodium signals caused by the shift reagent are such that several factors must be determined before the areas of the sodium resonances can be used to quantitatively follow the flux of sodium ions. These include the time constant for spin-lattice

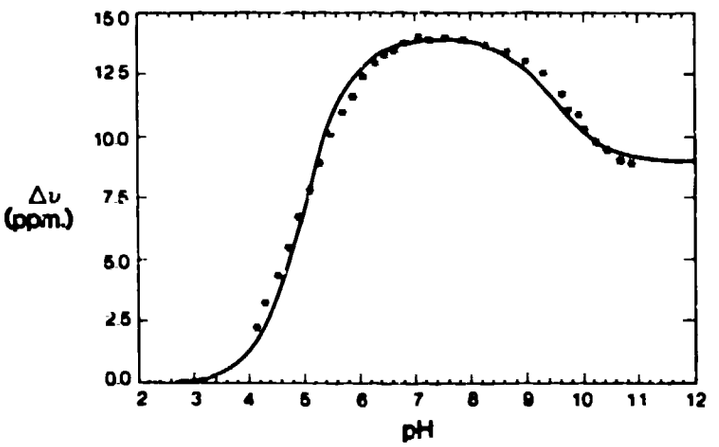

Fig. 2. Chemical shift difference between the DyTP-resolved sodium-23 NMR signals as a function of pH. The sample was a dual-compartment (coaxial) NMR tube, with 100 mM NaCl in one compartment, and NaCl + DyTP in the other in which the pH was varied with NaOH or HCl. The solid line is a fitted curve corresponding to two pKs, one of 5.0 and another of 9.5.

relaxation (T1), the extracellular pH, and the included and excluded volumes of the cells. We determined the sodium T1 to be 42 ± 0.6 ms in Linsameir and Skoog medium containing 195 mM sodium at a temperature of 292 K. The acquisition time for our data accumulations was 340 ms, so that the sodium nuclear spins reached thermal equilibrium after every pulse.

Binding of sodium to the DyTP is a complex process that is influenced by the pH of the solution (3). For this reason, the chemical shift difference between the two sodium resonances is a function of pH (Fig. 2). The data can be fitted to a two-site titration model with a span of 14.0 ppm and a pK1 of 5.0, for the first site, and a span of -5.0 ppm with a pK2 of 9.5 for the second. In the pH range from about 6.2 to 8.0 there is only a small change in the peak separation with pH; fortunately, this falls nicely around the range of biological interest. At a given pH the binding of sodium to the DyTP shift preagent follows a Michaelis-Menton saturable binding curve; at pH 7.8, 100 mM NaCl, the affinity was found to be 7.56 mM, with a

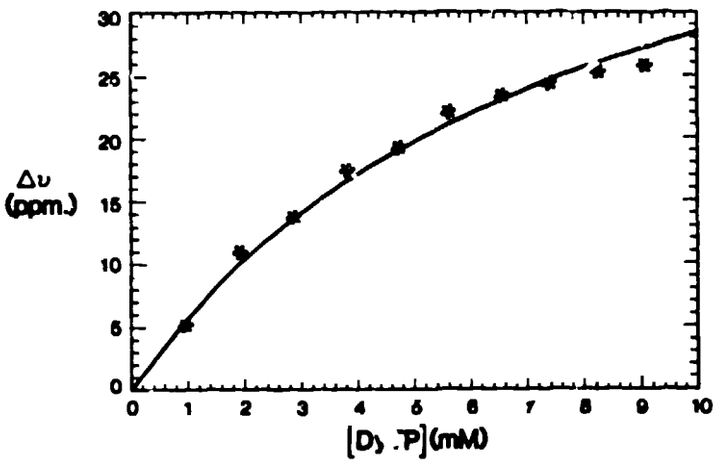

Fig. 3. Sodium binding to DyTP as measured from the chemical shift difference between two sodium signals from a sample similar to that described in fig. 2, in which the DyTP concentration was varied in one compartment. The solid line is a linear least squares fit to the data points of a saturation-binding curve with an affinity of 7.56 mM and a maximum splitting at infinite DyTP concentration of 50.0 ppm.

maximum splitting of 50.0 ppm (Fig. 3). Sodium is a quadrupolar nucleus (I=3/2, Q=0.12) so that any electric field gradient across the nucleus will distort the nuclear energy levels and cause the appearance of additional transitions that occur at higher and lower fields than those of the symmetric, rotationally averaged ion in solution. These other lines are not always easily observable and can give rise to a

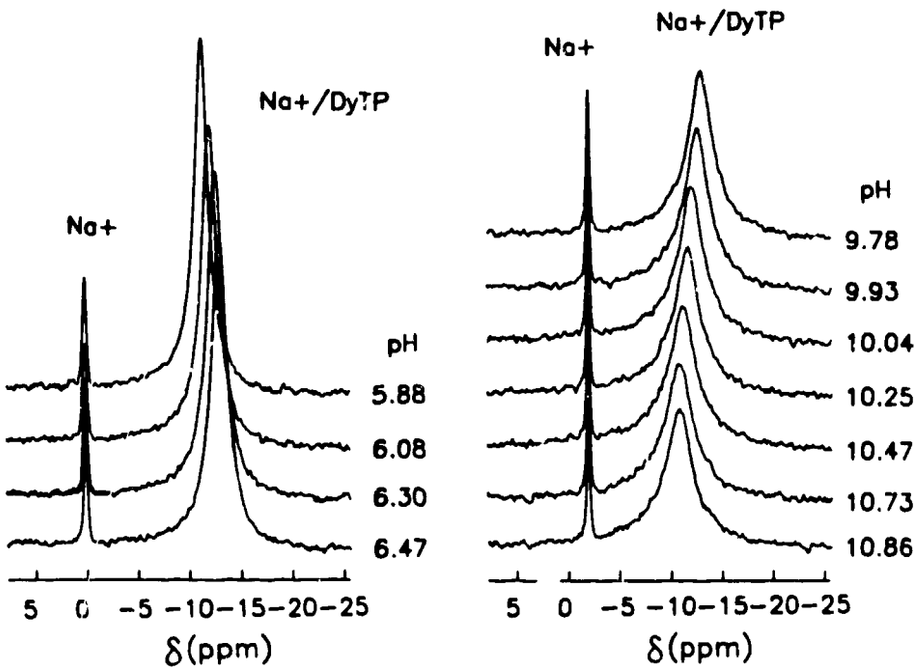

Fig. 4. Effect of pH on the sodium-23 NMR spectra of coaxial samples prepared as in Fig. 3, showing the variation of the splitting and linewidth of the DyTP-shifted signal.

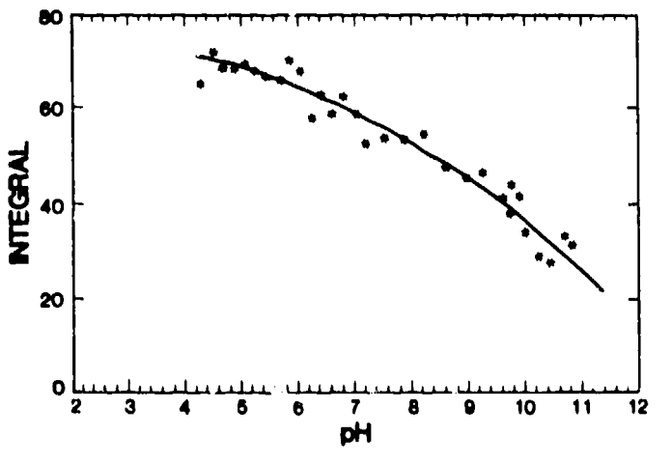

Fig. 5. Variation of the integrated intensity of fully-relaxed sodium-23 NMR signals in the presence of DyTP as a function of solution pH for data represented in Fig. 4.

spurious loss of intensity. This is what is seen for the signal of sodium bound to the DyTP as the pH is raised above about pH 6 (Figs. 4 and 5). Thus, one must be careful to control the pH of the medium during any experiments in which an accurate determination of the amount of sodium in the extracellular space is required. This is especially true for metabolising systems since they often excrete acids such as lactate or acetate into the medium during glycolysis. Adequate oxygenation must be maintained to prevent pH drift and loss of signal. Fortunately, the chemical shift difference between the two sodium signals serves as a sensitive monitor of changes in pH.

2.1 Sodium Efflux from Salt-Adapted Millet Cells

The process of adaptation of millet cells to a saline medium takes about a week for a shift to 130 mM NaCl. We examined the efflux of sodium from both adapted and non-adapted millet cells by means of Na-23 NMR and DyTP. The time dependence of the sodium resonances was measured during replacement of the external medium with an identical medium containing only half the sodium. The initial spectrum from a representative sample of NaCl-adapted cells is shown in Fig. 1A, while that for the same sample 90 min after the medium switch is shown in Fig. 1B. It is clear from the spectra in Fig. 1 that the cells lost sodium during the experiment; the kinetics of the sodium efflux are shown in Fig. 6 (open circles). The efflux curve could be fitted to the sum of two exponentials: $I(t) = 23.15 \exp(-t/9.15) + 76.85 \exp(-t/506)$, which implies that 23.15% of the intracellular sodium resided

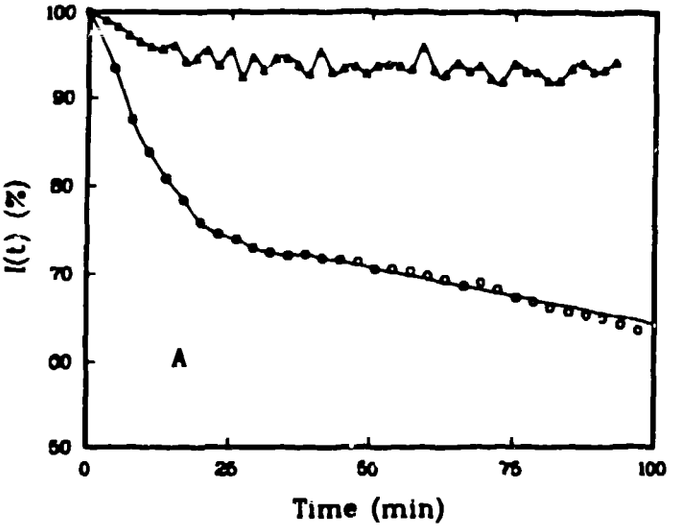

Fig. 6. Time dependence of the intracellular sodium concentration in suspensions of cultured millet cells as monitored by means of natural-abundance sodium-23 NMR. The circles represent efflux data obtained from cells adapted to growth on 130 mM NaCl, while the triangles represent data from non-adapted cells.

in a compartment which rapidly equilibrated with the medium, and that 76.85% of the intracellular sodium equilibrated at a much slower rate. By measuring the intracellular and excluded volumes of these cells (0.88 and 0.78 ml/g, respectively) we were able to calculate the two fluxes as 367 and 107 nmol Na/g/min for the faster and slower compartments, respectively at pH 6.7.

When non-adapted millet cells were loaded with sodium for a short time with respect to the time required for adaptation and tested using the same experimental protocol as above, a strikingly different pattern of sodium efflux emerged. There was very little sodium loss during the course of the experiment (Fig. 6, triangles) compared with the rates found for the adapted cells. In both of these cases, the extracellular pH was constant at 6.7 over 90 min as determined from the peak splitting. This is an indication that the DyTP was indeed not taken up by the cells and that our oxygenation of the cells was adequate to prevent medium acidification during the efflux period.

2.2 Sodium Influx into Millet Cells

The uptake of sodium by cells shifted from a medium containing no added sodium (about 1 mM) to one containing 130 mM NaCl is shown in Fig. 7. A linear least squares fit to the data from 6 experiments gave

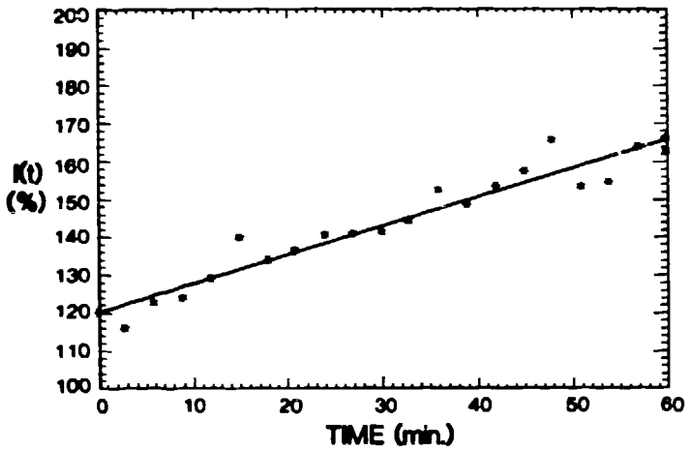

Fig. 7. Time dependence of the intracellular sodium-23 NMR signal for millet cells grown with 1 mM NaCl shifted to a medium containing 130 mM NaCl at time zero.

an influx of 0.757%/min. We measured the initial internal sodium concentration as 0.93 mM or 0.82 micromol/g. The larger statistical scatter evident in Fig. 7 arises from the smallness of the initial internal sodium signal, and its attendant poorer signal to noise ratio.

It is clear from the results presented above that both efflux and influx of sodium can be measured in living cells with good time

resolution from single samples of millet cells. We have extended these studies to include sodium transport in the roots of whole, hydroponically-grown, plants of the salt grass Distichlis spicata.

2.3 Sodium Transport in Roots from Intact Distichlis spicata Plants

The salt grass, Distichlis spicata, can grow in soil watered by saline solutions containing up to 500 mM NaCl. It is found in the playas of southern New Mexico, and in the salt marshes at Bodega Bay, California. We have obtained members of both of these populations and have grown individuals in the greenhouse using hydroponic technology in order to control the ionic environment surrounding the roots. We have used Na-23 NMR techniques as described above to monitor the transport of sodium out from and into the roots of these salt-adapted plants. The results illustrate another feature of NMR applied to living systems; we were able to perform multiple transport experiments on the same living plant.

2.4 Efflux of Sodium from Roots

When the roots from Distichlis plants grown in 130 mM NaCl-containing medium were quickly blotted and placed into an NMR tube containing medium with no added sodium (and 5 mM DyTP) the internal sodium moved out from the roots (Fig. 8). The kinetics of efflux are biphasic with time constants and compartment sizes similar to those found for the salt-adapted millet cells presented above: the equation

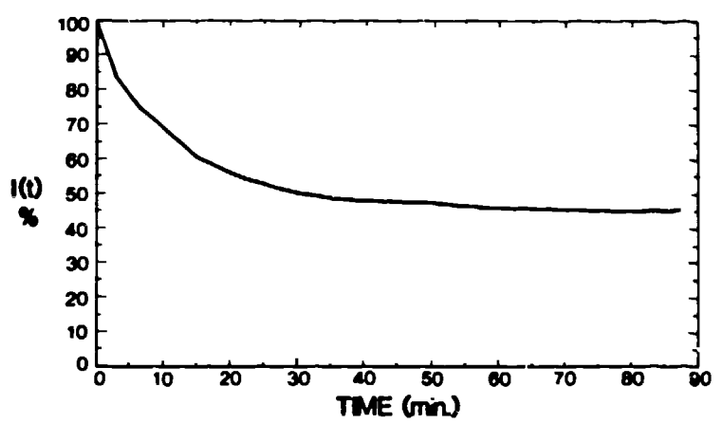

Fig. 8. Time dependence of the intracellular sodium-23 NMR signal for Distichlis spicata. Seen here is sodium efflux from the roots of this whole plant after the roots were placed into a medium containing 0 mM NaCl and 5 mM DyTP. In this and the following figure, the plants were grown hydroponicly on 130 mM NaCl and either washed extensively with sodium-free medium for the influx experiments, or placed directly into the NMR tube in sodium-free medium for the efflux runs.

describing the curve was found to be $I(t) = 48.8 \exp(-t/8.67) + 51.2 \exp(-t/771)$. Here the fast and slow compartments contained approximately equal amounts of sodium.

2.5 Influx of Sodium into Roots

After the efflux experiment was finished, we removed the medium bathing the roots and blotted the roots to remove clinging medium. Then, the roots were placed into medium with 5 mM DyTP and 130 mM NaCl in order to measure sodium influx. The movement of sodium from the medium into these roots was faster than that found for the millet cells (Fig. 9); the influx rate was found to be 4.95%/min, with a half-time of 10.1 min. No attempts have yet been made to transform these data into fluxes since the weight of the roots is not easy to measure without sacrifice of the plant.

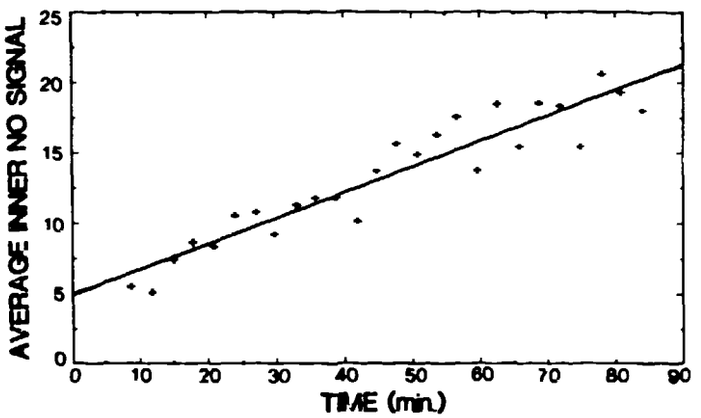

Fig. 9. Influx of sodium into the roots of a salt-adapted whole plant, Distichlis spicata, as monitored with the aid of real-time sodium-23 NMR.

These results represent the first demonstration that Na-23 NMR can be successfully utilized to measure the parameters of sodium transport in living systems in real-time, without invasion of the tissues of interest. We have shown that the rates, and amounts of sodium efflux correlate with the ability of a plant to adapt to saline stress in the environment. Sodium-23 NMR works well for this application because plants grown in a saline environment accumulate sodium and therefore give a strong intracellular sodium NMR signal. The relatively high sensitivity of the sodium-23 nucleus translates into an ability to measure much lower sodium concentrations, such as those found in mammalian cells.

2.6 Sodium content of Human Blood Cells

Normal human blood and parenchymal cells contain sodium at a concentration that is much less than that of blood. This concentration gradient across the cell membrane is maintained at the expense of cellular ATP by means of a (Na,K)-ATPase. With the high NMR sensitivity of sodium-23 one can still measure these low intracellular amounts of sodium. An example of such a measurement is shown in Fig. 10. Normal human blood (4 ml) from a 35-year-old female volunteer was

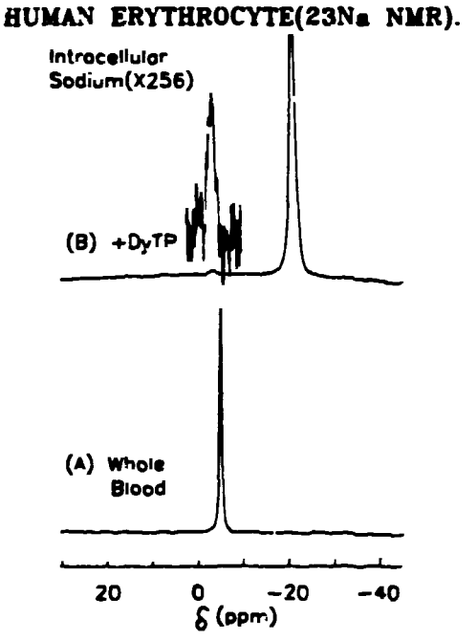

Fig. 10. Sodium-23 NMR spectra of (A) whole human blood and (B) whole human blood in the presence of DyTP showing the resolution of the sodium signal into intra- and extracellular fractions.

placed into a 10 mm NMR tube, and 0.2 ml of 100 mM DyTP was added. Spectrum A in Fig. 10 shows the sodium signal prior to the addition of the shift reagent. Atomic absorption analysis gave a sodium concentration of 138 mM for this sample. After the addition of the shift reagent (Fig. 10B) the extracellular sodium signal is shifted 17.93 ppm upfield, enabling the observation of the intracellular sodium signal. The relative integrals of these two signals were used to determine that these erythrocytes contained 5.1 mM sodium. The hematocrit for this blood sample was 52 $\pm$ 3%.

Human leukemic macrophages are another cell type to which we have applied the use of sodium-23 NMR. A sample of cells (125 million in 1.8 ml) was placed in a 10 mm NMR tube and oxygenated with a steady

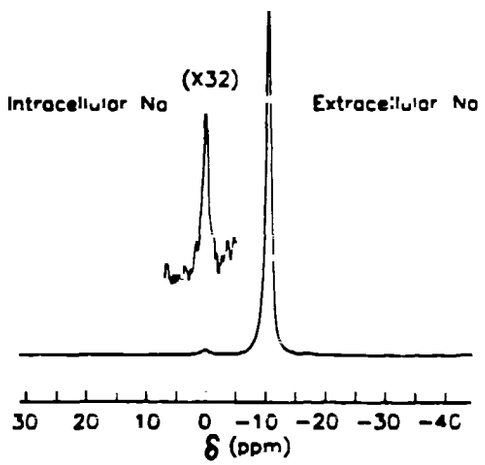

Fig. 11. Sodium-23 NMR spectrum of human leukemic macrophages in the presence of DyTP showing the intracellular sodium signal near 0 ppm.

stream of oxygen. After the addition of 5 mM DyTP the sodium spectrum (Fig. 11) shows two signals; the small signal downfield arises from the intracellular sodium, while the larger, upfield signal derives from sodium in the medium. Atomic absorption analysis gave a value of 165 mM sodium for this sample of cells suspended in phosphate-buffered saline. From the relative peak integrals we can estimate that these tumor cells contained 3.01 mM sodium or 43.2 femtomol Na/cell. These two studies demonstrate that sodium-23 NMR can be profitably used to measure the intracellular sodium concentration in living, human cells. We are now examining the transport of sodium in these human cell types.

3.0 CARBON-13 NUCLEAR MAGNETIC RESONANCE OF RAT ADIPOCYTES

Of all of the biologically important nuclides, carbon is the most interesting from the point of view of a biochemist or physiologist. Carbon forms the backbone of virtually all biomolecules; a complete description of intermediary metabolism would primarily consist of a map of the flow of carbon atoms from precursor foodstuff constituents into the product components of the cells and tissues of the organism. Indeed, there is no conclusive evidence that life itself is possible without the existence of carbon. For these and other reasons, the study of carbon biochemistry by a non-invasive, real-time technique would be of fundamental importance. Carbon-13 NMR has the needed potential to enable it to closely approach this ideal (4). The carbon-13 chemical shift range is large enough to provide superior spectral resolution compared to that of protons or phosphorus. The spectral dispersion is so great that virtually every carbon atom in a

moderately complex (molecular weight around 1000) biomolecule can be resolved. This implies that the metabolic transformations of biomolecules can be studied with essentially atomic resolution, i.e., one can map the flow of single carbon atoms through a pathway. The chemical shifts of carbon nuclei are sensitive to the formation and breakage of chemical (heteronuclear and homonuclear) bonds, and to the nature of hetero-, and homo-atom substituent bonds. Although C-13 is present in nature at an abundance of only 1.1%, isotopic enrichment techniques can provide a 100-fold increase in C-13 at specific sites in a molecule so that the metabolic transformation of particular carbon atoms can be studied against a substantially reduced or absent background of natural-abundance C-13. The sensitivity of C-13 is only 1.6% that of the proton, a fact that limits the detection of C-13 to concentrations in cells or tissues to around 1 mM with modern Fourier transform spectrometers. Polarization transfer techniques will no doubt lower this by one to two orders of magnitude in the next one to two years (5). Finally, the spin-spin coupling present between two bonded, magnetic nuclei like C-13 gives NMR a unique capability to monitor the integrity of carbon-carbon bonds.

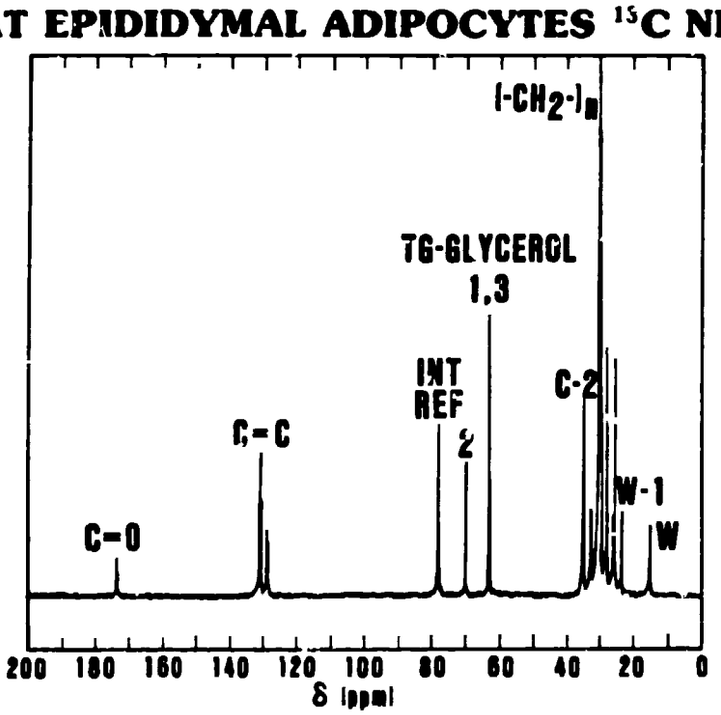

Fig. 12. A natural abundance, carbon-13 NMR spectrum of rat epididymal fat pad adipocytes. This spectrum was from 1 million cells with a signal averaging time of one minute. The excellent resolution of this spectrum provides discrete signals from almost every carbon in the triacylglycerol molecule.

3.1 Natural-Abundance C-13 NMR Spectrum of Rat Adipocytes

We have sought to use C-13 NMR to aid in the study of the hormonal regulation of adipose tissue metabolism, since this tissue plays an important, perhaps central, role in the etiology of diabetes and obesity. A natural-abundance, proton-decoupled, C-13 NMR spectrum of a suspension of rat, epididymal-fat-pad adipocytes is shown in Fig. 12. The spectrum can be completely assigned on the basis of published spectra of triacylglycerols and fatty acids (6). The signals can be assigned to 4 broad classes of carbon nuclei in differing environments as follows: methyl and methylene (14-35 ppm), esterified glycerol (62-70 ppm), unsaturated carbons (127-131 ppm), and carbonyls (172-174 ppm). Signals from the membranes or cytoplasm are not expected to be seen since they constitute less than 3% of the cell mass.

Important information regarding the sites and types of unsaturation of the fatty acyl side chains can be obtained rapidly from the NMR spectrum. Characteristic signals from olefinic sites appear in two places in the spectrum: near 130 ppm from the double bonded carbons themselves and in the methylene region near 30 ppm. The olefinic region of the spectrum is dominated, in this case from cells from rats given ad lib access to standard rat chow, by two signals separated by about 1.9 ppm. This separation arises from the magnetic inequivalence of olefinic carbon nuclei from monoenoic and polyenoic fatty acids. The carbon nuclei in oleic acid, for example, resonate at 130.51 and 130.76 ppm, while these same carbon nuclei in linoleate resonate at higher (128.73, 128.91) and lower (130.96 ppm) fields. Distinct signals from linolenate are seen at 127.84, 129.06, and 132.69 ppm; signals from the other three olefinic carbon nuclei in linolenate overlap those from oleate and linoleate.

The resonances from methylene carbon nuclei adjacent to olefinic sites are shifted away from the other methylene signals due to changes in their shielding arising from their olefinic neighbors. A signal at 23.35 ppm comes from penultimate carbon nuclei in the fatty acyl chain of linolenate. The peak at 26.35 ppm is indicative of an allylic carbon in a cis diene system; this could come from either linoleate or linolenate. The resonance at 27.92 ppm is characteristic of cis allylic carbon nuclei; this could arise from either oleate or palmitoleate. The resonance at 32.32 ppm is uniquely assigned to the second carbon from the methyl end of a dienoic fatty acid (6).

Certain features of these assignments have particular relevance with respect to the usage of C-13 NMR for metabolic studies on triacylglycerols. Upon esterification to a fatty acid, the signals from free glycerol (C1,3, 63.5 ppm; C2, 73.0 ppm) shift upfield sufficiently (C1,3, -0.8 ppm; C2, -3.1 ppm) so that free and bound glycerol can be easily resolved. This is an example of how C-13 NMR can be used to follow the integrity of the ester bond in triacylglycerols, and how, in a hydrolysis reaction, one could separately follow the esterified and free glycerol simultaneously. The chemical shift of the fatty acyl carboxyl carbon nuclei changes by -6.3 ppm upon methyl ester formation, and by another 1.3 to 2.6 ppm upfield upon esterification with glycerol, thus offering another independent

means for determining the integrity of the ester bond by C-13 NMR.

In order to make quantitative measurements of changes in the C-13 NMR signals from the adipocytes, it is necessary to know the spin relaxation and nuclear Overhauser enhancements for each resolved resonance. We have made these measurements (7) and have used them in the analyses of the data to be presented below. An integration of the spectrum of the adipocytes can be used to provide information about the types and amounts of fatty acyl chains present in the cells in a non-disruptive, and rapid fashion. The major fatty acids are palmitic (29.9%), oleic (27.9%), linoleic (34.1%), and linolenic (2.9%). Of the unsaturated fatty acids present, 53% are oleic, 45% are linoleic, and 2.7% are linolenic. These results agree within 2% with those found using gas chromatography.

3.2 Insulin Stimulation of [1-^{13}C]glucose Incorporation

One of the classical effects of insulin on the metabolism of the adipocyte is to stimulate the incorporation of glucose into the glycerol head group of the triacylglycerol. In separate experiments (data not shown) using [ul-^{14}C]glucose in the presence of 10 mM unlabeled glucose and 10 nM insulin, we found that adipocytes synthesized triacylglycerols at a rate of 330 nmol/million cells/hr. An average adipocyte contains from 1 to 10 nmol of lipid; this rate would then correspond to a change in the NMR signal integral of from 0.3 to 3%/hr. Changes of this magnitude are easily measured given the

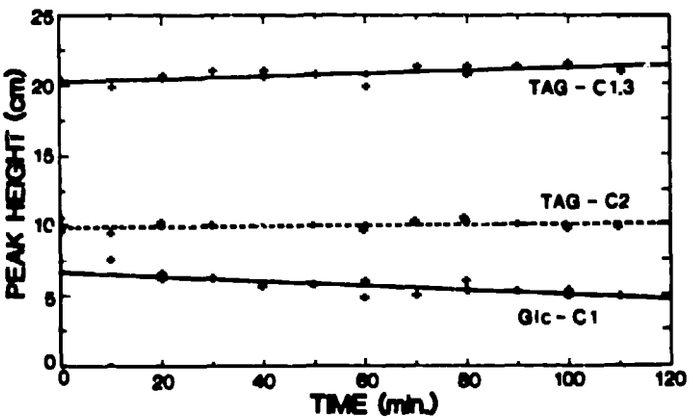

Fig. 13. Insulin-stimulated triacylglycerol synthesis from [1-^{13}C]-glucose in rat adipocytes monitored by means of carbon-13 NMR. One notes a decrease in the glucose signal, an increase in the signal from the triacylglycerol carbon 1,3 resonance, and no change in the signal from the triacylglycerol carbon 2. These changes are to be expected on the basis of the known flow of carbon from glucose to triacylglycerols.

very high signal-to-noise ratio obtainable from suspensions of about 1 million adipocytes.

When this experiment was repeated three times using C-13 NMR to detect the incorporation of glucose using 10 mM [1-^{13}C]glucose instead of the radioactive substrate, and 10 nM insulin, the results, at 310 K, show (Fig. 13) that the glucose was consumed by the adipocytes at a rate of 1.74 micromol/million cells/hr. The NMR signal from carbons 1 and 3 from the glycerol head group increased at a rate of 2.81%/hr, in substantial agreement with the data obtained above using C-14 glucose. The change in the total glucose signal during the course of this two-hour experiment was 1.7 times that found for the glycerol C1,3 signal. If all of the glucose was incorporated into the glycerol head group of the triacylglycerols the change in the glucose signal should have been equal to that for the glycerol signal. These data indicate that 43% of the added glucose was incorporated into other, unmeasured products including carbon dioxide and fatty acids. We have recently used sealed tubes containing hyamine to trap the evolved carbon dioxide and have found (data not shown) that there is significant labeling of the carbon dioxide. The rate of lipid synthesis shown in Fig. 3 was calculated to be about 1 micromol/million cells/hr.

The good resolution and dispersion of the C-13 NMR spectrum of adipocytes can be exploited in the present case to illustrate how certain resonances in the spectrum can be used as internal controls in order to check for systemmatic errors in the spectra from one time block to another. Labeling of carbon 2 of the glycerol moiety of the triacylglycerols will only occur if there is isotopic scrambling of the C-13, added at C1 of glucose, to C2 of glycerol-1-phosphate due to Kreb's cycle activity. There is a very minor flux through this route so that the glycerol C2 signal should be essentially constant over the course of the experiment. Any deviation from a slope of zero for the time dependence of this signal would have to arise from systemmatic effects such as floating of these very bouyant (density = 0.7) cells during the course of the experiment. The observed slope is 15.4 times smaller than that found for the glycerol C1,3 signal (0.374%/hr) providing good evidence for the absence of significant systemmatic errors in the application of this technique to the study of this process.

3.3 Isoproterenol Stimulated Lipolysis Using Natural Abundance C-13 NMR

The opposite process to that studied above is that of the breakdown of the ester bond of the triacylglycerols to form free fatty acids and glycerol. The adrenergic hormones, exemplified by epinephrine, control and promote this process. In our experiments probing the ad energic stimulation of lipolysis, the more stable analogue, isoproterenol, was used. Incubation of adipocytes with 5 μM isoproterenol resulted (Fig. 14) in the net hydrolysis of the ester bond, with the release of free fatty acids and glycerol (Figs. 14, 15, and 16). The initial time course of the changes in the lipid glycerol C1,3 signal (Fig. 15) shows that isoproterenol stimulated lipolysis

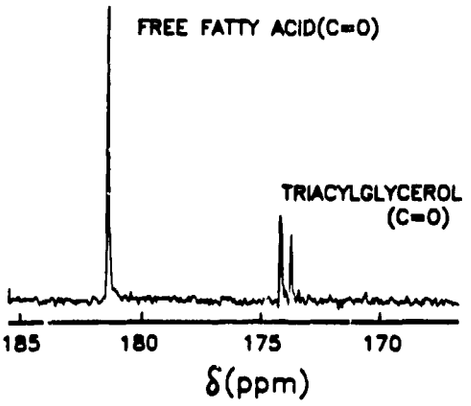

Fig. 14. Isoproterenol-stimulated lipolysis in rat adipocytes as determined by natural-abundance carbon-13 NMR. This is an example of the ability of carbon-13 NMR to provide information about the integrity of covalent bonds in biomolecules since the chemical shifts of the carbons vary according to their structure.

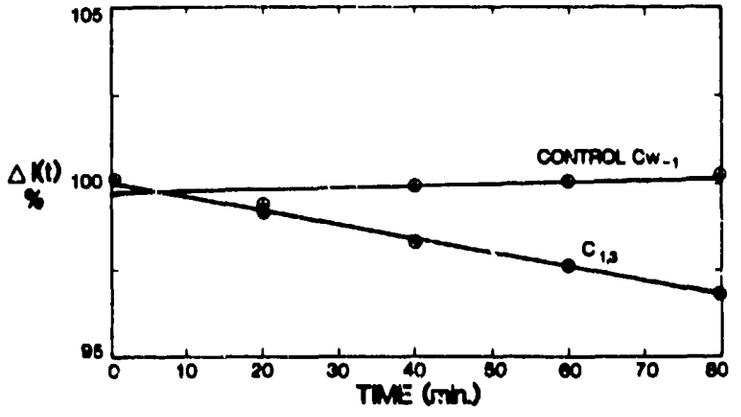

Fig. 15. Time course of isoproterenol-stimulated lipolysis in rat adipocytes as monitored by natural-abundance carbon-13 NMR. The control signals were from the penultimate carbon in the fatty acyl chain of the cellular triacylglycerols. The cleavage of the glyceride bond is shown as a decrease in the signal from the covalently-bound glycerol carbon 1,3 resonance.

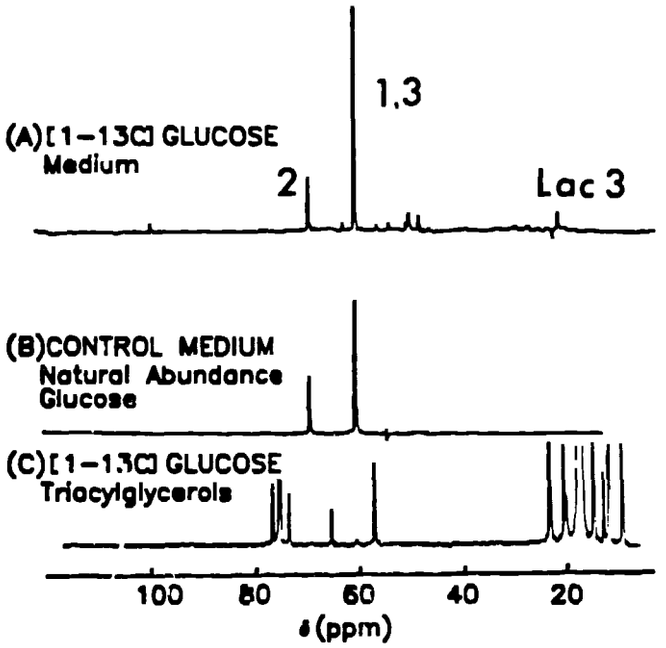

Fig. 16. Substrate cycling during lipolysis in rat adipocytes monitored by carbon-13 NMR. Adipocytes were incubated in the presence of 5 μM isoproterenol and either [1-^{13}C] or natural-abundance glucose. (A) In the presence of labeled glucose the cells produced glycerol in the medium with strong carbon-13 labeling at C1,3. (B) In the presence of natural-abundance glucose the ratio of the glycerol C1,3 peak to that of the C2 signal is 2:1 as expected from the random distribution of carbon-13. (C) With labeled glucose glucose the extracted triacylglycerols show a glyceride C1,3 to C2 signal ratio of 3.0.

stimulated lipolysis occurred at a rate of 2.4%/hr, a rate that is close to the rate found above for the synthesis of lipids. In Fig. 15 we have used another lipid signal as an internal control; the intensity of the resonance from the penultimate carbon in the fatty acyl chains has virtually zero time dependence. The decrease in the glycerol resonance intensity with time illustrates the fact that C-13 NMR can be used to monitor the breaking of chemical bonds, since the C-13 NMR frequency is different for the bound and free forms of glycerol. It also points out the usefulness of natural-abundance C-13 NMR for some purposes. It should be possible to apply these types of studies to humans, because the C-13 NMR spectrum, at natural-abundance, of a human arm (8) is completely dominated by signals from triacylglycerols.

3.4 Futile Cycling in Adipose Tissue

Carbon-13 NMR is capable of resolving virutally every carbon atom in most smaller biomolecules. Consequently, we can apply this

technique to the study of a very intriguing, and incompletely understood, facet of intermediary metabolism; a facet known as futile, or substrate, cycling. In this process, a precursor such as glucose which is labeled in a particular carbon position, is metabolized by a living system, and when the glucose pool is examined at a later time, it is found that there has been migration of the label to an initially unlabeled position. In most cases this label migration can be explained by the hypothesis that both anabolic and catabolic pathways operate simultaneously in the organism. A corollary of this hypothesis is that living systems "spin their wheels" so to speak, without doing as much useful work as the energy stored in the substrates would allow. In our work on carbohydrate metabolism in the rat liver (9) it was shown that futile cycling took place during glycogenesis at rates of from 40 to 100% of the theoretical maximum. Such high rates arose in that system because the pathways of glycogenesis and glycolysis are short and of comparable length. In the present case in the adipocyte, we sought to discover whether similar cycling took place over the longer metabolic distance from glucose to glycerol, and to measure the rates of lipogenesis during conditions favoring net lipolysis.

Adipocytes were incubated with 5 μM isoproterenol at 310 K under two conditions. For the control condition the cells were incubated with 10 mM natural abundance glucose. When all of the glucose had been consumed, the cells were separated from the medium. The triacylglycerols were extracted from the cells and dissolved in chloroform for C-13 NMR examination. C-13 NMR spectra were also taken from the medium. For the other condition, an identical aliquot of cells was incubated with the addition of 10 mM [1-^{13}C]glucose as the only differing variable. The results (Fig. 16) show several interesting features. There was substantial natural abundance glycerol release during the incubation of the control cells (Fig. 16B). Glycerol released during incubations with [1-^{13}C]glucose was labeled at C1,3 (Fig. 16A), indicating that it arose from the [1-^{13}C]glucose in the medium, rather than from lipolysis of existing triacylglycerols. The extracted triacylglycerols (Fig. 16C) showed the same labeling pattern as the glycerol (Fig. 16A). Isoproterenol stimulated glycolysis as shown by the appearance of lactate in this case and not in the control samples.

The addition of isoproterenol is classically thought to inhibit the uptake of glucose and at the same time, to stimulate lipolysis. Our results show that it does indeed stimulate lipolysis, while at the same time accelerating glycolysis. These results can be interpreted in two ways. The first is that triacylglycerols are made in the adipocyte in a first-in, first-out fashion, so that the newly made lipid molecules are the first to be hydrolyzed. This model would be appropriate for glycogen where glucosyl residues are added one at a time to precursor polymeric strands, but it is extremely unlikely for adipocytes since triacylglycerols exist as a lipid droplet without structure within the cell. The second possibility is that lipogenesis and lipolysis take place simultaneously within the adipocyte. We strongly favor this as the explanation for the labeling pattern seen

for the medium glycerol in both experiments (Fig. 16 A and B) This second model is the only one which is consistent with the appearance of labeled lactate in the isoproterenol-treated cells (Fig. 16A). It may be necessary to propose new, and more significant, roles for adipose tissue in the body; that of a metabolic buffer for energy regulation, and as a significant producer of lactate and glycerol as substrates for hepatic gluconeogenesis.

4.0 POLYSACCHARIDE SYNTHESIS IN PLANT CELLS

The initiation of cell wall polysaccharide synthesis is an important obligatory first step during the process of regeneration of plant tissue from protoplasts. In order to optimize regeneration procedures a method for the monitoring of polysaccharide formation in vivo would be of considerable interest. We have used ^{13}C NMR combined with ^{13}C labeled substrates to follow the biosynthesis of cellulose and other α-glucans and glucuronoarabinoxylans in real time, in situ, within the cells of suspensions of proso millet, a monocot.

Suspensions of proso millet (Panicum miliaceum) were derived from a single callus regenerated in protoplast culture (1, 10). Exponentially growing cells (1.5 g) were harvested by filtration and suspended in a buffer of 50 mM KH_2PO_4 at a pH of 5.5 containing 50% D_2O. Proton-decoupled, ^{13}C nuclear magnetic resonance spectra were obtained with the aid of a Bruker WM300wb spectrometer operating at 75 MHz for carbon. A control natural-abundance spectrum was accumulated for 30 min from the oxygenated cell suspensions. At this time 18 mg of [1-^{13}C, 90%]-D-glucose was added and additional spectra were accumulated in 30 min blocks. For the isolation of a cellulose-enriched polysaccharide fraction other portions of cells were adapted to growth on glucose as their sole carbon source, and then cultured for 3 weeks with fresh medium containing the ^{13}C labeled substrate. During this time the cell mass tripled. Alkalai-insoluble cellulose was prepared by means of the extraction procedure of Carpita (11) and suspended in D_2O for NMR measurement.

4.1 High Resolution ^{13}C NMR Spectrum of Cellulose

In plant cells cellulose exists as a crystalline chains of β (1->4)-linked poly-D-glucose whose degree of polymerization ranges from 2,000 to 14,000 (12). From NMR studies of cello-oligosaccharides and other glucose-containing oligosaccharides (13, 14) it is expected that C1 from glucose will resonate at 103 ppm. The ^{13}C NMR spectrum (Fig. 17) of a cellulose-enriched fraction of cell wall polysaccharides isolated from millet cells grown on labeled glucose shows a major signal at 103.2 ppm which we assign to C1 of β-glucosyl residues in cellulose. This signal has a full width at half maximum of 270 ± 30 Hz which corresponds to an average mass of about 270 kD based on the dependence of T_2 and rotational correlation time on Stoke's radius and mass. This corresponds to a degree of polymerization of about 1,500 residues, a value which is at or below the lower limit estimated by

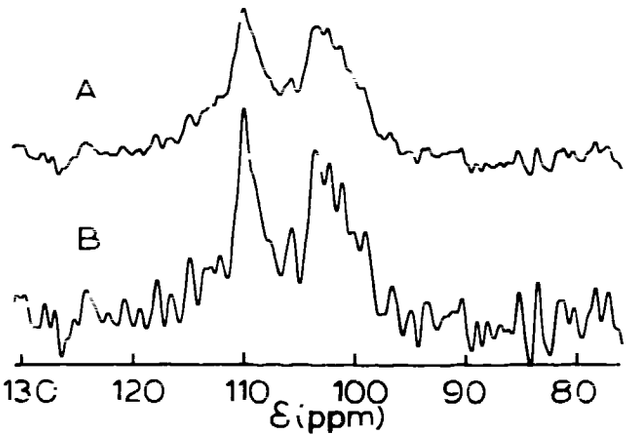

Fig. 17. Proton-decoupled ^{13}C NMR spectrum at 75.412 MHz of cellulose purified from P. milliaceum cells grown for three weeks in 0.2 M [1-^{13}C]-D-glucose. (A) Spectrum processed with 40 Hz digital filtration; 37,687 scans; acquisition time, 0.508 sec; pulse width, 90° (20 μs); temperature, 303K. (B) The same data as for (A), but processed with Gaussian multiplication for resolution enhancement with -40 Hz line broadening and a peak time of 5.1 msec. The primary signals arise from C1 of β-glucans and glucuronoarabinoxylans.

Marx-Figini (12). Our extraction process may have degraded the chains somewhat in length. Native cellulose should have a ^{13}C nuclear resonance width of between 370 and 2,500 Hz rendering it more difficult to observe.

The other prominent ^{13}C nuclear resonance, in the spectrum from the [1-^{13}C]-glucose fed cells, at 108.4 ppm arises from the anomeric carbon from L-α-arabinosyl residues in the glucuronoarabinoxylan which copurifies with the cellulose. We expect to find the signals from the anomeric carbon of the β(1->4)-linked xylosyl residues at a field position of about 102 ppm (14). The signal in Fig. 17 at 103.2 ppm has a shoulder around 102.6 ppm which could be the resonance from this carbon. Both L-α-arabinose and β-D-xylose are biosynthesized from D-glucose in millet cells, with preservation of C1 labeling.

4.2 β-glucan Synthesis from [1-^{13}C]-glucose *in vivo*

The natural-abundance, proton-decoupled ^{13}C NMR spectrum of millet cells (Fig. 18) shows signals from both structural and metabolic components. The strongest signals arise from sucrose. These cells were grown on 0.11 M sucrose, washed extensively, and resuspended in sample buffer without sucrose. Thus it is likely that these sucrose signals originate from within the cells. Sucrose hydrolysis takes place in these cells when transferred to a sucrose-free medium (Fig.

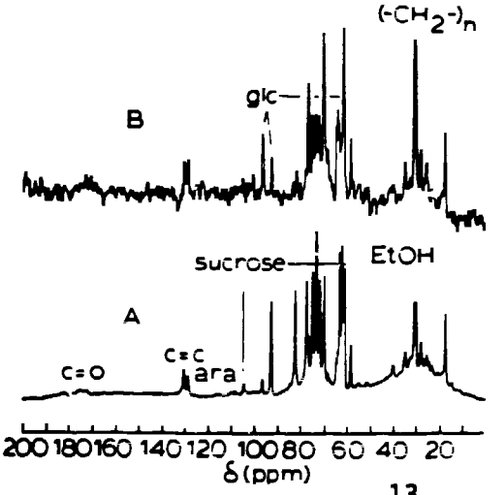

Fig. 18. Proton decoupled, natural-abundance ^{13}C NMR spectra of 1.5 g of protoplast-derived suspension cultures of P. milliaceum cells suspended in D_2O. (A) Cells grown in 4% sucrose, 37,349 scans with a 90° (20 μs) pulse and an acquisition time of 0.508 sec. (B) The same sample as in (A) after 7 days growth in new, sucrose-free medium containing 4% glucose, 826 scans in 7 minutes.

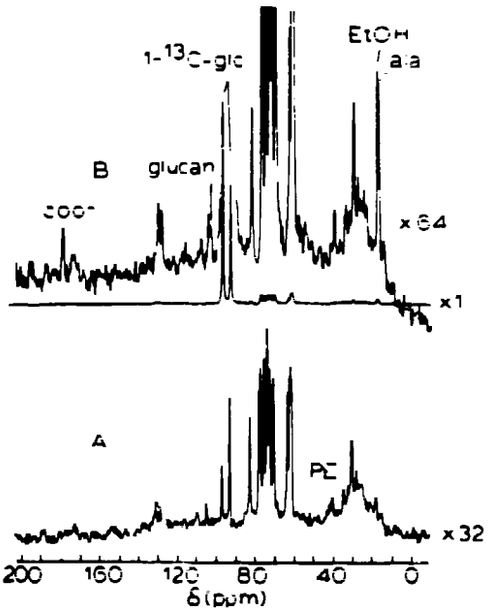

Fig. 19. (A) Natural-abundance, proton-decoupled ^{13}C NMR spectrum of P. milliaceum cells grown for 3 weeks on natural-abundance glucose (0.2 M). This spectrum was taken as a control run for 30 min, with 12,324 scans using a 25.2° (5.6 μs) pulse. (B) ^{13}C NMR spectrum of the same cells as in (A) 90 minutes after the addition 50 mM [1-^{13}C (90%)]-D-glucose.

18B). When cells were incubated in this way for 7 days, about 75% of the intracellular sucrose was hydrolyzed to glucose.

In order to follow β-glucan synthesis in these cells, we adapted cells to growth on glucose by switching the carbon source from sucrose to glucose. The cells grew equally well on the glucose. Incubation of these cells with 18 mg [1-^{13}C]-glucose in the NMR tube resulted in the synthesis of a compound with a chemical shift of 103.1 ppm (Fig. 19, 20) which we identify as a β-glucan, which is most likely cellulose. The rate of increase in this signal was constant (Fig. 21); from the slope of the time course plot we can estimate that these cells made cellulose at a rate of about 0.5 μmol-glc/g-cells/hr. The width of this signal is 103 ± 10 Hz, or about 2.7 times smaller than that found for the equivalent signal in the ^{13}C NMR spectrum of the cellulose-enriched fraction presented above. This difference in the linewidths probably arises from the differing positions of labeling likely to occur in the two different cases. The chronic feeding experiment would be expected to have labeled a large fraction of the total cellulose residues with ^{13}C, but the acute biosynthesis experiment would have emphasized end labeling. Terminal glucosyl residues would be expected to be much more mobile than those located closer to the center of the chains.

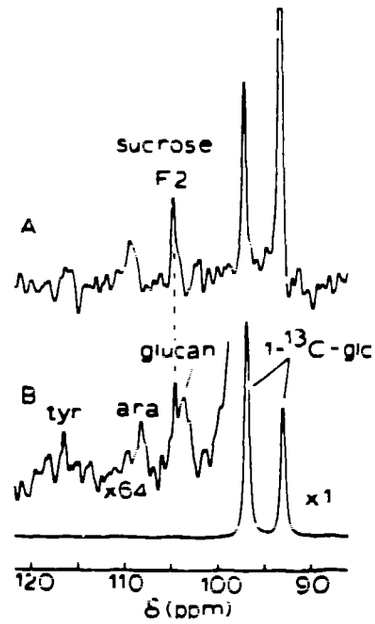

Fig. 20. An expansion of the polysaccharide anomeric carbon region of the ^{13}C NMR spectra shown in Fig. 19. (A) Control spectrum taken of the P. milliaceum cells for 30 min prior to ^{13}C-labeled substrate addition. (B) Spectrum taken 90 min after the addition of 50 mM [1-^{13}C (90%)]-D-glucose. Note the labeling of the β-glucan signal and its resolution from that of sucrose F2.

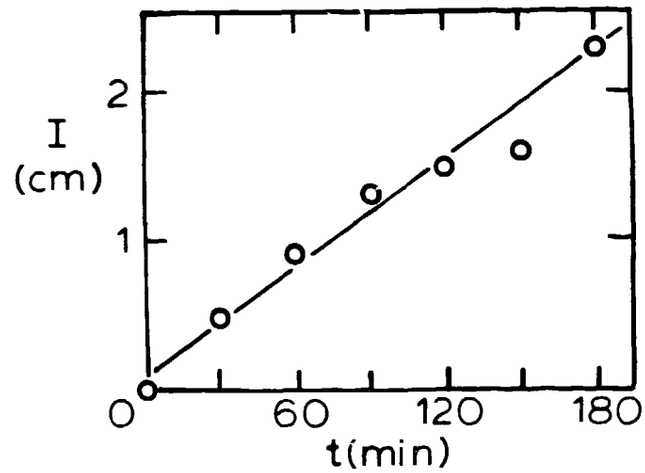

Fig. 21. Time course of β-glucan synthesis after the addition of 50 mM [1-^{13}C (90%)]-D-glucose to a suspension of protoplast-derived suspensions of P. milliaceum cells.

These experiments demonstrate that the synthesis of cell wall polysaccharide material in plant cells can be monitored in situ, in real time in the cells of moncots by means of ^{13}C NMR and ^{13}C labeling of substrates. It will now be possible to study the regulation of this process and its relation to the regeneration of callus tissue from protoplasts. These studies are underway along with studies of the structure of various alkalai-extractable cell wall fractions by means of high resolution proton and ^{13}C NMR as well as with GC-MS.

This work was done under the auspices of the United States Department of Energy.

5.0 REFERENCES

1. Sillerud, L. O. and Heyser, J. W. Plant Physiol. 75 (1984) 269.

2. Gupta, R. K. and Gupta, P. J. Magn. Reson. 47 (1982) 344.

3. Chu, S. C., Pike, M. M., Fossel, E. T., Smith, T. W., Balsano, J. A., and Springer, C. S. J. Magn. Reson. 56 (1984) 33.

4. Shulman, R. G., Brown, T. R., Ugurbil, K., Ogawa, S., Cohen, S. M., and Den Hollander, J. A. Science 205 (1979) 160.

5. Sillerud, L. O., Alger, J. R., and Shulman, R. G. J. Magn. Reson. 45 (1981) 142.

6. Batchelor, J. G., Cushley, R. J., and Prestegard, J. H. J. Org. Chem. 39 (1974) 1698.

7. Sillerud, L. O., Han, C. H., Francendese, A. F., and Bitensky, M. W. J. Biol. Chem. (in press).

8. Alger, J. R., Sillerud, L. O., Behar, K. L., Gillies, R. J., Shulman, R. J., Gordon, R. E., Shaw, D., and Hanley, P. E. Science 214 (1981) 660.

9. Sillerud, L. O. and Shulman, R. G. Biochemistry 22 (1983) 1087.

10. Heyser, J. W. Z. Pflanzenphysiol. 113 (1984) 293.

11. Carpita, N. C. Plant Physiol. 72 (1983) 515.

12. Marx-Figini, M. In: Cellulose and Other Natural Polymers, R. M. Brown (Ed.) Plenum, New York (1982) 243.

13. Gast, J. C., Atalla, R. H., and McKelvey, R. D. Carbohydr. Res. 84 (1980) 137.

14. Sillerud, L. O. and Yu, R. K. Carbohydr. Res. 113 (1983) 173.